1	Water compositional evolution around an historic asbestos mine,
2	Troodos Mountains, Cyprus
3	
4	Aled D. Evans ¹ , Dave Craw* ² , Joanna L. Shannon ¹ , Joseph Hattersley ¹ , Lewis J. C. Grant ¹ ,
5	Rosalind M. Coggon ¹ , and Damon A. H. Teagle ¹
6	1. School of Ocean and Earth Science, National Oceanography Centre Southampton,
7	University of Southampton, Southampton, UK
8	2. Department of Geology, University of Otago, P.O. Box 56, Dunedin 9054, New
9	Zealand
10	*Corresponding author: <u>dave.craw@otago.ac.nz</u>
11	
12	Abstract
13	The historic Amiantos chrysotile asbestos mine (closed 1988) in the Troodos mountains, is
14	hosted in serpentinites that constitute the Artemis Diapir. Host rocks were extensively sheared
15	and brecciated during Pleistocene-Holocene diapiric uplift, enabling penetration of meteoric
16	waters. Veins of serpentine minerals, especially fibrous chrysotile, have formed throughout
17	this uplift history with accompanying carbonates, and carbonate surface precipitates that form
18	at spring sites. The Artemis Diapir is juxtaposed by faults against less-permeable partially
19	serpentinized peridotites of the Olympus Diapir that forms the highest elevation (1952 m) of
20	the Troodos Mountains. Streams and shallow groundwater draining the Artemis Diapir have
21	high concentrations of Mg ²⁺ and dissolved inorganic carbon (DIC), minor Ca ²⁺ , and pH 8-10.
22	In addition, these waters have high concentrations of Na ⁺ , K ⁺ , Cl ⁻ , SO ₄ ²⁻ and trace elements Cs,
23	Ba, Br, B, and Li sourced from the dissolution of mineral inclusions in the host serpentinites.
24	These dissolved constituents overprint low levels of marine aerosols that occur in local
25	meteoric precipitation. Passage of surficial waters through asbestos mine tailings have locally
26	enhanced dissolution of these elements because of even higher permeability and small particle
27	size that resulted from mine-related comminution. All surficial waters are strongly
28	supersaturated with respect to chrysotile (log $Q/K = 3-9$) and carbonate minerals, especially
29	magnesite (log Q/K = 1-2). Evaporative carbonate precipitates form episodically on stream
30	beds and tailings surfaces during dry seasons. Erosion of mine tailings and friable host rocks

by rain events in the steep mountain environment contributes detrital chrysotile asbestos to

stream sediments, with potential for aeolian remobilization. The relatively high abundance of

carbonates already in the rocks and mine residues, combined with carbonate and chrysotile

31

32

supersaturation in surficial waters, limits the efficacy of these materials for CO₂ capture through enhanced weathering and mineral carbonation.

36

37

34

35

Keywords: chrysotile; carbonate; magnesite; brucite; mine drainage; water quality

38

39

40

41

42

43

44

45

46

47

48

49

50

51

52

53

54

55

56

57

58

59

60

61

62

63

64

65

66

67

Introduction

Large chrysotile asbestos mines were developed in several serpentinite terranes around the world in the 20th Century, although most of these mines have since closed (Ross and Nolan 2003). These mines were focused on coarse fibrous chrysotile asbestos that is predominantly hosted in veins. Chrysotile is a polymorph of the hosting serpentine; thus there is little chemical difference between the ore, waste rock and tailings, and the surrounding serpentinite terranes. Chrysotile asbestos fibres typically contain elevated Cr, Ni and Co as trace metals of potential toxicity in the environment (Bloise et al. 2024). Surrounding serpentinites are also well-known for their elevated Ni and Cr contents, and the asbestos mine sites are similar (Meck et al. 2006; Apollaro et al. 2011, 2019; Kumar and Maiti 2015; Duivenvoorden et al. 2017; Gwenzi 2020; Jaques and Pienitz 2022). Chrysotile mine drainage waters generally do not have dissolved constituents that lead to negative environmental implications, unlike, for example, sulfidic mines that can generate acid mine drainage (AMD) and/or discharges with anomalously elevated metal levels (Charalambides et al. 2003; Meck et al. 2006; Lottermoser 2010). Consequently, chrysotile asbestos mine drainage chemistry has received relatively little research compared to these more environmentally significant sites and their discharges (Meck et al. 2006; Kumar and Maiti 2015; Gwenzi 2020; Jaques and Pienitz 2022; Bloise et al. 2024). However, mobilisation of particulate asbestos has been considered to be a potential environmental issue (Daghino et al. 2009; Emmanouil et al. 2009). Conversely, there has been substantial recent interest in the geochemistry of ultramafic mine sites, with numerous studies investigating their potential for carbon capture through enhanced weathering and mineral carbonation (Kelemen and Matter 2008; Wilson et al. 2009; Kelemen et al. 2011; Oskierski et al. 2016; Lechat et al. 2016; Bullock et al. 2021; Paulo et al. 2023).

Most large chrysotile asbestos mines around the world were developed in old tectonically quiescent ultramafic terranes in areas of low relief (e.g., Australia, eastern Canada, Russia, southern Africa; Ross and Nolan 2003; Meck et al. 2006; Lechat et al. 2016; Oskierski et al. 2016). In contrast, the Amiantos asbestos mine of Cyprus described in this study was developed in serpentinites that crop out at high altitudes (>1000 m) in the tectonically active Troodos Mountains.(Fig. 1a-c; Wilson 1959; Evans et al. 2021). The mine and hosting rocks

occur in an area of steep relief and deeply incised valleys on the margin of the ~2 km high Mt Olympus near the crest of the mountain range (Fig. 1a-c). The hosting serpentinites have been extensively sheared and brecciated by diapiric extensional deformation and associated uplift that is still occurring, albeit slowly (~1 mm/year; Morag et al. 2016; Evans et al. 2021). Consequently, there has been abundant incursion of meteoric water in to the rock mass (Fig. 1d), resulting in extensive water-rock interactions (Evans et al., 2024a). In this study, we describe the results of these water-rock interactions in the vicinity of the asbestos mine and in the associated mine tailings.

Our study focuses on evolution of major ion concentrations, and some trace elements, in surficial waters in streams and associated shallow groundwater springs and seeps that drain the mine tailings and brecciated diapiric host rocks. Our study complements studies of deeper groundwaters in the Troodos Mountains, some of which are hyperalkaline and most of which occur in surrounding mafic host rocks at progressively lower elevations (Neal and Shand 2002; Christofi et al. 2020). We compare our surficial water compositions to deeper but low-volume hyperalkaline waters (pH 11-13) in the same serpentinite host in which the mine occurs (Neal and Shand 2002; Christofi et al. 2020; Evans et al. 2024a). As such, this study complements a parallel study that focuses on evolution of the hyperalkaline waters (Evans et al. 2024a). Studies of hyperalkaline waters in ultramafic rocks have highlighted the presence in these waters and their host rocks of some fluid-mobile elements (e.g., K, Na, Cl) that are not normally associated with ultramafic terranes (Scambelluri et al. 1997; Neal and Shand 2002; Apollaro et al. 2011; Chavagnac et al. 2013; Leong et al. 2021; Evans et al. 2024a). In this study we focus on these fluid-mobile elements (e.g., Table 1) and the compositional evolution of waters in the asbestos mine and the surrounding natural streams. As such, we address mobility of elements other than those more commonly associated with ultramafic rocks, such as Cr and Ni (Apollaro et al. 2011, 2019; Bloise et al. 2024). In addition, we evaluate the widespread carbonate dissolution and precipitation associated with these waters from the perspective of carbon sequestration via enhanced rock alteration in natural and mine-induced fragmental serpentinite rocks.

97 General setting

68

69

70

71

72

73

74

75

76

77

78

79

80

81

82

83

84

85

86

87

88

89

90

91

92

93

94

95

96

98

99

100

101

The Amiantos asbestos mine (Fig. 1b-d) was active between 1908 and 1988, with large-scale excavation and processing operations beginning in the 1950s. The mine site grew to be >2 km wide, with a central open pit surrounded by piles of tailings ~200 metres high (Fig. 1b-d). After closure in 1988, the site was abandoned for several years before a remediation programme,

including revegetation (Fig. 1c), was initiated in early 21st Century and remains on-going. The open pit area has undergone most rehabilitation, with some reprofiling of mine benches and channelling and collection of run-off water into a central lake. This rehabilitated area is adjacent to a popular tourist visitor centre for the Troodos Geopark that occupies an old mine building. The mine and surrounding areas have been incorporated into the Troodos National Forest Park, where roadside picnic areas and walking tracks have been developed. Despite this extensive rehabilitation activity, large areas of peripheral tailings deposits remain unvegetated, and water runoff from these tailings discharges into natural streams. These tailings waters and the surrounding natural streams are the principal topic of this study.

The Amiantos asbestos mine is hosted in highly sheared and fragmented serpentinite of the Artemis Diapir (Fig. 1d; Evans et al. 2021). This diapiric body, and the adjacent less deformed Olympus Diapir, constitute the exposed portions of the ultramafic component of the Troodos Ophiolite that dominates the central portion of Cyprus (Fig. 1a,d; Moores and Vine 1971). These variably serpentinised peridotites form the highest parts of the Troodos Mountains, including the highest point at Mt Olympus (1952 m; Fig. 1a,b). The sheared, fractured and friable rocks of the Artemis Diapir (Fig. 2a-e) occur at slightly lower altitudes (>1000 m to 1765 m) than the Olympus Diapir (>900 m to 1952 m) (Fig. 1d) but are still higher than surrounding Troodos ocean crustal rocks and submarine sediments. Hence, streams draining these diapirs flow over serpentinite only, simplifying the interpretation of water chemistry in this study.

Outside the asbestos mine, the Artemis Diapir landscape is partially covered by open conifer forest with abundant areas of unvegetated bare ground (Fig. 2a-e; Supp. Fig. S1), especially on steep slopes. Today, diapiric uplift and erosion are occurring at similar rates (Evans et al. 2021), and most slopes are covered with active talus and debris flow material (Fig. 2a-e; Supp. Fig. S1). Many streams are deeply incised into fresh but friable rocks and the associated active talus slopes (Fig. 2a-e; Supp. Fig. S1), with lower relief forested interfluves. Stream beds consist of cobbles of serpentinite with interstitial serpentinite sand.

The Troodos Mountains and Cyprus in general have a Mediterranean climate, with cool wet winters and long hot (up to 40°C) summers (Fig. 1a, inset; Charolambides et al. 2003; Griggs et al. 2013; Le Coz et al. 2016). The crest of the mountains receives a coating of snow in winter and minor snowfalls can extend to the levels of the asbestos mine site. Occasional afternoon thunderstorms interrupt otherwise rainless periods in the summer months. However, evaporative processes dominate the surficial environment in summer and autumn, causing stream beds to become dry. Springs emanating from hillside outcrops and talus deposits are

variably active in early summer after winter rains but most of these wane or completely dry up during summer, leaving minor precipitates (Fig. 2e; Supp. Fig. S1, S2).

Methods

Water samples were collected in late spring (May 2019 and 2023) as stream flows waned from the winter rains. Some small dry stream beds were followed upstream to reach flowing water. An initial set of 16 samples of waters flowing on serpentinite in 2019 was collected for regional context for a study of hyperalkaline waters (Evans et al. 2024a), A single sample of snow from the crest of the Troodos Mountains was collected in March 2020 as part of this regional context. An additional set of 13 samples was collected in 2023 specifically for this study, with focus on the general vicinity of the asbestos mine. However, no samples were collected from within the open pit in either sampling campaigns, to avoid possible confounding run-off from fertiliser that was applied during the site revegetation activities.

Samples were filtered on site (0.45 μ m) and divided into four aliquots, with no head-space, for separate analysis of cations, anions, dissolved inorganic carbon (DIC), and stable oxygen and hydrogen isotopic analyses. Prior to geochemical and isotopic analyses, samples were prepared and processed in a Class 100 Clean Laboratory suite in the Centre of Earth Research and Analysis (CERAS) of the Geochemistry Research Group, National Oceanography Centre Southampton (NOCS), University of Southampton.

Major and minor cation concentrations (e.g., Table 1) were measured by inductively coupled plasma-source mass spectrometry (ICP-MS; Thermo X-Series II) in the Geochemistry Research Group of the University of Southampton. Si, B and Li were not measured in the second sample set. Anion (Cl, SO₄, and Br) concentrations were measured by ion chromatography (Thermo Aquion Ion Chromatography System) and DIC was measured by VINDTA 3C (Marianda) at NOCS. The δ^{18} O and δ D of the first set of waters were analysed at the Scottish Universities Environmental Research Centre (SUERC) in East Kilbride, UK. Details of field sampling, laboratory sample preparation, and analytical methods and associated standardisations are provided in a supplementary document attached to Evans et al. (2024a) and are not repeated herein.

Minerals and their textures were identified primarily with standard thin section petrography, augmented with spot analyses and element mapping on polished sections with a scanning electron microscope and energy dispersive analytical attachment (SEM-EDS) and undertaken at NOCS using a Carl Zeiss Leo1450VP Scanning Electron Microscope (SEM)

coupled to an Oxford Instruments Energy Dispersive X-ray Spectroscopy (EDS) X-act-10mm² silicon drift detector utilising the Aztec energy software. Typical SEM operation conditions were 20 kV at a working distance of 19 mm.

Additional element mapping of a polished thick section was undertaken with a laser ablation (LA) system (Elemental Scientific Lasers NWR193 Excimer with a TwoVol2 ablation cell; Bozeman, MT, USA) coupled to an Agilent (Agilent Technologies Inc., CA, USA) 8900 Triple Quadrupole inductively coupled plasma mass spectrometer (LA-QQQ-ICP-MS; Evans et al. 2024b). Sampled surficial mineral precipitates were characterised with X-ray diffraction (XRD), SEM-EDS, and/or ICP-MS analysis. Typical laser settings are reported in Evans et al. (2024b)

Geochemical analyses of serpentinised peridotite, variably deformed serpentinite breccias, and serpentine veins including chrysotile veins, were determined for an in-depth study of trace element distribution and redistribution in Olympus and Artemis Diapirs (Evans et al. 2025*; Evans et al., 2024c). Rock and mineral analytical methods are described in Evans et al. (2025) and data are available attached to that publication (Evans et al., 2024c).

Geochemical modelling of water-mineral relationships was done with the Geochemists Workbench® software package. Phase diagrams of relative mineral stabilities were calculated with program Act2. Dissolved ion speciations were determined with program SpecE8. Associated mineral saturation indexes (log Q/K) for dissolved ions in the waters were also calculated with SpecE8, with equilibrium saturation at log Q/K = 0; supersaturated minerals >0, and undersaturated minerals <0. Minerals unlikely to form at 25°C were pruned from the resultant output to leave a list of plausible minerals (e.g., Table 2) that could theoretically directly precipitate (log Q/K >0) and also minerals that could precipitate during subsequent evaporation (log Q/K <0).

Results

195 Rocks and minerals

The Artemis Diapir consists almost entirely of serpentinite (Table 2). The most intact outcrops consist of blocks of hard but serpentinised peridotite (1 to 10s metres), with no remnants of primary peridotite minerals. These more robust serpentinite rocks are surrounded by variably sheared and brecciated serpentinite (Fig. 1d; 2a-e). This fragmented serpentinite, which dominates the Artemis Diapir landscape, has been extensively recrystallised and veined by several generations of serpentine. Some bodies of rock at outcrop scale are dominated by veins and recrystallised serpentine with only minor remnants of the original serpentinised peridotite.

Veins include the chrysotile asbestos that was the focus of mining in a portion of the diapir but is also common outside the mined area (Fig. 2c,d). Physical redistribution of eroded serpentinite debris, including vein chrysotile asbestos, dominates natural streams draining across the Artemis Diapir (Supp. Fig. S1).

Tectonic fragmentation associated with diapiric rise has formed complex breccia zones (Fig. 2a-e) that include cm-dm scale serpentinite fragments, cataclasites (mixed cm to mm scale fragments) and gouges (soft, mm to μm scale fragments). Veins and cements of carbonate minerals accompany serpentine veins in the breccias, cataclasites and gouges (Fig. 2a,c,d; Table 2). These are mostly calcite but some aragonite and magnesite occur as well. Many carbonate veins cut across older serpentine veins, but some outcrops have sets of mutually cross-cutting serpentine and carbonate veins, and some carbonate-cemented breccias have late-stage chrysotile veins cutting across them (Fig. 2d; Supp. Fig. S2). Accessory magnetite and rare pyrrhotite accompany some serpentine generations, and accessory andradite (Ca₃Fe³⁺₂Si₃O₁₂) is common, especially in late-stage serpentine veins (Table 2). Freshly eroded rocks are green and unoxidised, but some stable outcrops and stream boulders have brown coatings of ferric oxyhydroxide (Fig. 2a-c).

Whole rock analyses show elevated concentrations of a range of light elements compared to typical mantle peridotites (Evans et al. 2024b; 2024c; 2025), as exemplified by Na and K (Fig. 3a). Concentrations of these elements are highly variable, with breccias and veins showing greater variation than the solid serpentinised peridotite blocks (Fig. 3a-d). Chromium, one of the dominant minor elements in the serpentinites, has limited variation in the cores of hard rocks, much wider variation in the breccias, but generally low concentrations in veins (Fig. 3b). In detail, these solid rock cores comprise serpentine phases pesudomorphing original olivine and pyroxene grains (Fig. 3c,d). There are also differential trace element distributions in secondary minerals pseudopmorphing primary minerals with, for example clear differences between B and Li distributions (Fig. 3c,d). Subsequent vein generations have caused substantial overprinting and some redistribution of these trace elements (Fig. 3c,d).

Evaporative carbonate-rich precipitates are common on all dry stream beds and damp brecciated outcrops, typically coating the serpentinite clasts with a white veneer (Fig. 2e; 4d; Supp. Fig. S3-S6). Local precipitate aprons and travertine deposits have developed where spring waters have emerged and persistently evaporated (Supp. Fig. S3). Evaporative deposits sufficiently large to sample were mostly calcite, some of which was Mg-bearing and with traces of Fe. Aragonite and magnesite precipitates have also been identified but are less common. Rare brucite precipitates, some with evaporative halite, have developed where hyperalkaline

spring waters mix with surficial waters on drying outcrop and talus surfaces (Supp. Fig. S1; Evans et al. 2024a). However, these latter precipitates and associated waters are volumetrically minor and are not considered further in this study apart from their use for comparative purposes.

Amiantos mine hydrogeology

Rocks within the asbestos mine are essentially the same as those outside the mine in the Artemis Diapir, but show more evidence of diapir-related shear deformation, brecciation and fragmentation, and are more extensively veined, especially with chrysotile asbestos and carbonate minerals (Fig. 2d; 4a,b). Mine tailings (Fig. 4c-e) are mineralogically the same as these outcrops but particle sizes have been reduced through mine extraction and crushing. The chrysotile asbestos content is lower because of mine-related liberation and extraction to leave minor, albeit widespread, fibrous asbestos residues (Fig. 4d,e). The mine tailings deposits also include some unprocessed serpentinite boulders, cobbles and pebbles that were separated from the asbestos-rich material during processing (Supp. Fig. S4, S5). Most tailings clasts exposed at the surface have at least some carbonate coatings (Fig. 4d,e).

The mine tailings were dumped to form flat-topped piles with marginal slopes at angle of repose (~30°) for the debris (Fig. 4c) and these slopes have consolidated with a hard surface crust enhanced by annual wetting and evaporation cycles. Rainwater runoff runnels (cm-dm scale) are locally incised into this crust. In addition, deeper gullies are spaced at 10-100 m scale across the slopes and these are the locus of active erosion during rain events. Tailings have been reworked down these gullies to form outwash fans that have discharged into adjacent streams (Fig. 4c; Supp. Fig. S4, S5). The fans have variable sedimentary differentiation, with a finely particulate component (fine sand, silt and associated chrysotile fibre clusters) travelling farthest to form low relief pans that can be further remobilised into nearby streams (Fig. 4c; Supp. Fig. S4, S5). These fine pans develop hard crusts, locally with evaporative carbonate cement, when they dry and they are then crossed by desiccation cracks (Supp. Fig. S4, S5). As a result of this physical remobilisation, abundant serpentinite debris and some chrysotile asbestos have contributed to the sedimentary deposits on the nearby stream beds (Fig. 4f). Surficial carbonate precipitates are abundant downstream of the mine tailings deposits where tailings have been physically remobilised, and where discharging water seeps are evaporating (Fig. 4f; Supp. Fig. S4, S6).

The mine tailings are sufficiently permeable to allow passage of shallow groundwater, which emerges as seeps and springs from the lower slopes of the main tailings piles and flows into natural streams during the wet seasons (Supp. Fig. S4, S5). The discharges wane or

completely dry up during dry seasons. Tailings that have partially filled a natural valley have dammed the stream to form a lake that receives some seepage waters (Fig. 4c). This lake fills in winter when incoming stream discharges are higher than the rate of drainage through the tailings (Supp. Fig. S6). The lake drains during the summer as the input waters dry up, leaving a bed of finely particulate tailings. Evaporative carbonate deposits are especially common on dried surfaces in the vicinity of this lake (Supp. Fig. S6) and downstream of the tailings piles that dam the lake (Fig. 4f). These evaporative deposits redissolve during wet seasons and are typically absent in early spring.

Principal water components

The δ^{18} O and δD of surficial serpentinite stream waters reflect their meteoric origin by lying on or close to the local Cyprus meteoric water line (Fig. 5a). The data spread along that line and are arrayed around the Troodos snow data point (Fig. 5a). Similarly, the analysed mine waters also plot close to the Troodos snow, on the meteoric water line and in the middle of the range of surrounding stream waters (Fig. 5a). In contrast, the hyperalkaline spring waters have distinctly different δ^{18} O and δD compositions and plot far off the meteoric water line (Fig. 5a) indicating significant fluid-rock isotopic exchange.

Most streams draining the ultramafic regions of the Troodos massif have moderate Na $^+$ and Cl $^-$ concentrations (<500 µmol/kg) that are slightly above the marine aerosol content of the Troodos snow (<250 µmol/kg; Fig. 5b). There is a general trend of these ions increasing in tandem in less dilute stream waters, and the mine waters follow this same trend (Fig. 5b). This trend is broadly parallel to that of the seawater ratio, but with higher Na $^+$ (Fig. 5b). The most concentrated mine waters have salinity about half that of seawater (Fig. 5b). The hyperalkaline spring waters are even more concentrated along a broadly similar trend (Fig. 5b). Potassium and sulfate concentrations in most stream waters are low (<50 µmol/kg; Fig. 5c). However, the mine waters show a strong positive trend for increase in both these ions, especially K $^+$ which is >600 µmol/kg in the two most concentrated mine waters, and this trend of increasing concentrations is distinctly different from the seawater ratio (Fig. 5c). The hyperalkaline springs have higher concentrations of both K $^+$ and sulfate than the mine waters, but lie on a subtly different trend from that of the mine waters (Fig. 5c).

Magnesium is strongly elevated (>2500 μ mol/kg) in streams and mine waters compared to the more dilute streams, with mine waters having generally higher Mg²⁺ than most stream waters (Fig. 5d,e). One sample of mine water seeping from tailings had extremely high Mg²⁺

(BU1; Fig. 1b; 5d,e; Table 1). These generally high Mg²⁺ concentrations contrast strongly with the relatively low Mg²⁺ in the hyperalkaline springs (Fig. 5d,e). In contrast, Ca²⁺ is relatively low (<200 μmol/kg) in most stream and mine waters compared to the hyperalkaline springs. All stream and mine waters had very high DIC (>4000 μmol/kg) with the highest concentration in the tailings seepage sample BU1 (Fig. 5e,f; Table 1). In contrast, most hyperalkaline springs had lower DIC than the surface waters (Fig. 5e,f).

310

311

304

305

306

307

308

309

- Trace elements in waters
- Despite the high Cr in the host serpentinites, dissolved Cr is low in all waters (<1 µmol/kg) and is only slightly enriched in mine waters compared to most stream waters (Fig. 6a). Likewise, dissolved Fe concentrations are low (<5 µmol/kg) in stream and mine waters (Fig. 6a). Dissolved Ba is low with a wide range in stream waters (Fig. 6b). The mine waters show
- evolution towards higher Ba with sulfate in a trend that is different from that of the hyperalkaline springs (Fig. 6b). Similarly, Cs is low and variable in stream waters, with a trend
- of increasing Cs with sulfate that is different from that of the hyperalkaline springs (Fig. 6c).
- 319 Lithium and boron also show similar patterns of enrichment in mine waters with increasing
- sulfate (Fig. 6d,e). Br has increased slightly in mine waters broadly in parallel with increasing
- 321 Cl⁻ (Fig. 6f) as is expected for a halogen. However, this correlation is weak, the data are highly
- variable, and several analyses were below detection ($\sim 10~\mu mol/kg$) for stream and
- 323 hyperalkaline spring waters (Supp. Table S1). Al, Mn, Rb and Sr were low (<1 μ mol/kg) and
- variable in analysed waters (Table 1; Supp. Table S1). Pb concentrations were mostly below
- detection limit of 10⁻⁶ μmol/kg or only marginally above that level (Table 1; Supp. Table S1).

326327

Discussion

- 328 Mine water compositional evolution
- Many of the fluid mobile elements that are dissolved in mine waters have concentrations
- similar to, or even higher than, concentrations in the stream waters (Fig. 5b-f; 6b-e). The
- elevated Si concentrations, along with some of the dissolved Mg, have probably been derived
- from dissolution of serpentinite, the principal silicate in the rocks. The specific sources for
- many of the other elements, such as Na, K, Cl, Cs, Ba, and Br, are not known, but they have
- been apparently inherited from the peridotite precursors to the Artemis Diapir serpentinites
- 335 (Fig. 3a-d; Evans et al. 2024a; 2025). Elevated sulfate may have been partly derived from initial
- serpentinization of peridotite (Alt et al. 2012), possibly with a contribution from alteration of
- the minor accessory pyrrhotite, Similar primary elemental enrichments have been described

from the Oman ophiolite (Leong et al. 2021), whereas Scambelluri et al (1997) report Clbearing hydrous minerals and high-salinity fluid inclusions in association with serpentinised peridotite. The elemental maps for B and Li in serpentinite from the Artemis Diapir (Fig. 3c,d) suggest that these have then been variably redistributed to different serpentine vein generations. Similar redistribution processes may have affected the other light elements (Evans et al. 2024a), but potential sources for most of these elements have not been identified petrographically.

The hyperalkaline fluids have been effective at extracting the light elements (apart from Mg) from the rocks, and/or at resisting dilution, compared to the stream and mine waters, resulting in consistently high concentrations (Fig. 5b,c,f; 6a-f). Mine waters have higher concentrations of these elements than the stream waters and form general enrichment trends from those surficial waters. These evolutionary trends for mine water compositions are different from, and do not converge with, the hyperalkaline spring water compositions (Fig. 5b,c,f; 6a-f). These observations, combined with the hydrogeological settings of the mine waters and associated mixing trends between groups (Fig. 6b,c), preclude the elevated mine water compositions arising from mixing of surface waters with hyperalkaline waters (Evans et al. 2024a). The stable oxygen and hydrogen isotope data (Fig. 5a) also support the clear separation of mine water compositional evolution from the hyperalkaline spring waters. We conclude that the mine waters have evolved from surficial meteoric waters via enhanced waterrock chemical interactions within the mine-derived materials, probably because of the greater comminution of these mine-derived materials in initial outcrops and especially in the tailings (Fig. 4a-d); Supp. Fig. S4-S6).

Carbonate dissolution and precipitation

Carbonate minerals are prominent components in the serpentinite host rocks and veins, in the mine-related debris, especially the mine tailings (Fig. 4d-f). Evaporative carbonates are common on rock and tailings surfaces and on stream beds, as temporary deposits during dry seasons. Consequently, Mg²⁺, Ca²⁺ and DIC are major components of stream waters and evolved mine waters (Fig. 5d-f). Calcite is the most common carbonate mineral identified in the underlying rocks, although aragonite is locally present as well. However, water analyses indicate that dissolution of Mg-bearing carbonate is the dominant chemical process in the surficial environment (Fig. 5e). The resultant Mg²⁺:DIC ratio generally parallels the stoichiometric 1:2 molar ratio expected for magnesite dissolution, including that for the BU1 tailings seepage sample (Fig. 5e; Table 1). Magnesite is supersaturated in all the waters (Fig. 7a; Table 2).

Hydromagnesite (Mg₅[CO₃]₄[OH]₂.4H₂O) is a common product of serpentine carbonation (Wilson et al. 2009; Thom et al. 2013; Oskierski et al. 2016; Paulo et al. 2023), and hydromagnesite is close to equilibrium saturation in Artemis Diapir streams and mine waters (e.g. sample BU1; Table 2). However, the observed Mg²⁺:DIC ratio does not fit a predicted stoichiometric ratio for hydromagnesite dissolution although some data, especially the mine waters, do spread towards that ratio (Fig. 5e). Likewise, the observed low dissolved Ca²⁺ concentrations result in substantial deviation from the stoichiometric 1:2 molar ratio expected for calcite dissolution (Fig. 1b; 5f; Supp Fig. S6). Nevertheless, calcite is supersaturated in all waters (Fig. 7a).

Catchment-wide carbonate mineralogy is clearly complex. With only few exceptions, the Mg²⁺, Ca²⁺ and DIC in mine waters do not show an evolutionary trend towards higher concentrations, as does occur for many other elements (Fig. 5b,c; 6b-f). Our combined field and geochemical observations suggest that all the waters, while supersaturated with carbonate components, have been involved in periodic dissolution and precipitation of carbonate minerals in the various surficial environments (Fig. 2e; 4b-f; 7a; Supp. Fig. S4-S6). The exact carbonate minerals, or combinations of minerals, are not known but several potential Mg-Ca carbonate minerals are close to or above saturation in these waters (e.g., Table 2). These minerals could precipitate during surficial evaporation and redissolve in wet seasons (Supp. Fig. S4-S6).

Other potential dissolution and precipitation reactions

The presence of significant levels of dissolved silica, along with the elevated Mg²⁺ in all the surficial waters attests to dissolution of serpentine, and the waters are strongly supersaturated with respect to chrysotile (Fig. 7b; Table 2). There is no evidence for formation of the clay minerals saponite or sepiolite (Fig. 8a; Table 2) in even the most tectonically comminuted rocks of the diapir (e.g., Fig. 2e). The mine waters have intermediate levels of chrysotile supersaturation in comparison to the stream waters, rather than showing more advanced chemical evolution (Fig. 7b). We have seen no direct evidence for precipitation of serpentine in the mine tailings or stream sediments, although traces of such precipitation could occur during evaporation (Table 2).

There is widespread evidence for serpentine precipitation in late-stage veins throughout the rock mass during the longer term (Pleistocene-Holocene) development of the Artemis Diapir (Fig. 2a-d; 3c,d). A longer-term approach towards equilibration between rock minerals and near-surface waters is depicted in Fig. 8a, where the observed surface water compositions straddle the serpentine dissolution boundary. Some paragenetically late-stage serpentine veins

are intergrown with carbonates, are mutually cross-cutting with carbonate veins, or are clearly crosscutting carbonate-cemented breccias (Fig. 2d; Supp. Fig. S2), attesting to localised fluctuations across this equilibrium boundary at times (Fig. 8a). The time scales for completion of the apparently reversible serpentine carbonate reaction (Fig. 8a) are not known, but low-temperature authigenic chrysotile has been shown to develop with carbonate minerals over 5 ka (Craw et al. 1987).

Serpentinite in the Artemis Diapir contains minor iron as Fe²⁺ in solid solution (<5 wt%; Table 2; Evans et al. 2025). Iron has been mobilised to a small extent in solution in the stream and mine waters (Fig. 6a; Table 1). Oxidation of ferrous to ferric iron is essentially instantaneous in alkaline waters (Langmuir 1997). Hence, the amount of iron in solution is controlled principally by precipitation of ferric oxyhydroxide (e.g., Fe[OH]₃ precipitate; Fig. 7c). The solubility of ferric iron in this system is sensitive to water redox potential, and the arbitrary value chosen for Fig. 7c merely provides an illustration of this equilibrium setting in relation to the observed data. During Pleistocene evolution of the Artemis Diapir, some iron may have remained as Fe²⁺ in solid solution in the abundant carbonate minerals or brucite, and some ferric iron has partitioned into andradite, magnetite, or pyroaurite during formation of various generations of serpentine veins (Fig. 8b; Plümper et al. 2014; Ellison et al. 2021). Ferric iron has the potential to mobilise Cr from the rocks into streams and groundwaters (Apollaro et al. 2019).

Evaporation to complete dryness of stream and mine waters must result in seasonal precipitation of a wide range of minerals (e.g., Table 2), although many of these precipitates will be volumetrically trivial, and will redissolve in wet seasons. Halite and brucite (Table 2) have been identified in spring precipitates from mixed surface and hyperalkaline waters (Evans et al. 2024a). Despite the abundant dissolved sulfate, no evaporative sulfate minerals have been detected this far, although some mine waters have Ca²⁺:sulfate ratios indicative of stoichiometric dissolution of gypsum (Fig. 7d). It is likely that at least some of the common white evaporative precipitates contain minor gypsum and epsomite (Table 2).

Environmental significance

The Amiantos mine, especially the tailings piles, are major visual landscape features, but the physical and mineralogical nature of the mine materials are essentially identical to the surrounding natural Artemis Diapir (Fig. 1b; 8c). The tailings have undergone additional comminution during mine processing, and some increases in porosity and permeability were associated with deposition (Fig. 4b-e; 8c). They now have a significant component of fine

materials, including chrysotile asbestos fibres, that are readily mobilised into streams by reworking during rain events (Fig. 4c,f; Supp. Fig. S3, S4). However, none of these processes are different from the natural processes that have occurred in the Artemis Diapir throughout its Pleistocene-Holocene history of tectonic uplift, fragmentation, and erosion (Supp. Fig. S1, S2). Tectonic comminution of the serpentinite has been locally more extreme than mine processing (e.g., Fig. 2a-e), and on-going natural erosional processes are similar to deposition and reworking of the tailings (e.g., Supp Fig. S1).

The physical end-results of both natural erosion and erosion of tailings includes similar redistribution of chrysotile asbestos in streams (Fig. 4f; Supp. Fig. S1). Hence, while detrital asbestiform chrysotile in streams is considered to be an environmental hazard (Ross and Nolan 2003; Emmanouil et al. 2009), this issue is naturally widespread across the Artemis Diapir rather than just focused on the mine wastes from which most asbestos was removed by mine processing. Likewise, wind-blown chrysotile asbestos may emanate from dry stream beds and hillsides during summer in both natural and mine waste settings. However, the low-relief pans of finely particulate tailings outwash (Fig. 4c; Supp. Fig. S3, S4) contain some fine asbestiform chrysotile, and when dry these pans could constitute an aeolian environmental hazard that is not replicated in the natural environment.

The comminution, porosity, and permeability of the tailings have been responsible for enhanced water-rock interactions that have led to some higher dissolved concentrations of a range of elements compared to surrounding streams (Fig. 5b,c; 6a-f; 8c). Seepages from the tailings piles have dissolved loads that reach half seawater concentrations of, for example, Na and Cl locally during the onset of dry seasons (Fig. 5b,c). Nevertheless, these elevated water concentrations are still lower than those of the natural hyperalkaline springs that emanate from the diapir (Fig. 5b,c; 6a-f; Evans et al. 2024a). Since the tailings seeps are largely seasonal and low-volume, their contributions to the environment are relatively minor compared to the more dilute natural streams.

Carbon sequestration

Ultramafic rocks, including chrysotile asbestos mine tailings, have been investigated as sinks for atmospheric CO₂ via enhanced alteration processes that precipitate carbonate minerals (Kelemen and Matter 2008; Wilson et al. 2009; Kelemen et al. 2011; Oskierski et al. 2016; Lechat et al. 2016; Bullock et al. 2021; Paulo et al. 2023). One such reaction potentially involves formation of Mg-carbonates (e.g., Table 2) from serpentine (e.g., chrysotile carbonation; Fig. 7a; Thom et al. 2013). Our observations in the Artemis Diapir in general

indicate that the tectonic uplift and associated deformation and fragmentation have been effective at encouraging chemical interactions that have led to precipitation of carbonate minerals from serpentine alteration throughout the rock mass (Fig. 2e; 5e,f; 7a; 8a-d; Supp. Fig. S2). There are associated high levels of supersaturation of carbonate minerals and serpentine in the stream waters (Fig. 7a,b; 8a). Similar processes, including similar levels of carbonate and serpentine supersaturation in mine waters, have occurred in the mine area, especially where evaporation has caused ephemeral seasonal carbonate-dominated precipitation and re-dissolution (Fig. 4f; 8c,d; Supp. Fig. S3, S5). The common occurrence of carbonate in the diapir, as precipitates and in solution, suggests that carbon sequestration has already been active in natural geochemical processes during Pleistocene-Holocene evolution of the diapir (Fig. 8a-d).

Further reaction of serpentinite to form carbonate is hindered by the widespread coatings of carbonate on rock surfaces (Fig. 4a-f). This armouring of potentially reactive rock surfaces, and the resultant decrease in reactivity of the rock mass (Oelkers et al. 2018, Emmanuel 2022) is well-known in the mining industry where efficiency of passive water treatment systems decrease with time (Lottermoser 2010; Matthies et al. 2010). Natural erosion and mine-related comminution have undoubtedly created some fresh serpentinite surfaces for further carbonate formation (Fig. 4c-f). However, surficial carbonate films inherited from Pleistocene processes, combined with seasonal precipitation of extra armouring layers, will counteract some of the CO₂ sequestration processes in the tailings (Fig. 4d,e). Our conclusion is that enhanced alteration processes in serpentinites can be effective for sequestering CO₂ but in the case of the Artemis Diapir and the Amiantos mine tailings, these processes have already been widespread in the highly fragmented rocks, and there may be limited capacity on human time scales without further comminution to expose fresh serpentine surfaces (Fig. 8d).

499 Conclusions

The Amiantos chrysotile asbestos mine in Troodos Mountains, Cyprus, is undergoing rehabilitation and revegetation, but large volumes of mine tailings remain unremediated. These tailings consist of carbonate-bearing serpentinite debris that ranges from boulders to silt in size, and includes some remnants of chrysotile asbestos. The tailings have been locally reworked into fans that extend into nearby streams, contributing sediment that includes chrysotile asbestos to those streams. However, the surrounding host rocks, which constitute the actively rising and eroding Artemis serpentinite diapir, are mineralogically and physically similar to the

mine tailings and similar sediments, including chrysotile asbestos. These materials are also being contributed to natural streams across the rest of the diapir.

Streams and shallow groundwater draining the diapir have elevated Mg²⁺ and dissolved inorganic carbon (DIC), minor Ca²⁺, and have pH 8-10. These waters have dissolved unusual light-element bearing mineral inclusions in the hosting serpentinite to release Na⁺, K⁺, Cl⁻, SO₄²⁻ and trace elements Cs, Ba, Br, B, and Li at higher levels than are contributed by marine aerosols in local meteoric water. Water passing through the mine tailings have evolved to even higher concentrations of these elements because of enhanced interaction with finer particles that resulted from mine-related comminution (Fig. 8c). Some waters seeping from tailings at the beginning of the summer dry season have salinities near to that of seawater (Fig. 5b,c), and evaporative carbonate-rich precipitates are common in dry seasons.

All surficial waters are strongly supersaturated with respect to chrysotile and carbonate minerals, especially magnesite (Fig. 7a,b). Water-rock equilibria may have been maintained in the long term (Pleistocene-Holocene) to support carbonation of serpentine and associated sequestration of atmospheric CO₂ (Fig. 7a; 8d). However, the high levels of mineral supersaturation mean that this carbonation reaction could be reversed at times, and the complex history of serpentine vein formation attests to this possible reversal. Hence, the abundance of carbonates already formed over geological time in the rocks and mine residues, combined with carbonate and chrysotile supersaturation in surficial waters, limits the efficacy of these materials for modern carbon sequestration purposes.

Declaration of Competing Interests

The authors declare that they have no known competing interests.

Data availability

- All data used in this study are provided in the text and cited sources, and Supplementary data
- files for this article can be found online at: **link to be provided on acceptance

Acknowledgements

- We thank the Geological Survey Department of the Republic of Cyprus for facilitating field
- work. Funding for this research was provided from a Natural Environment Research Council-
- 538 SPITFIRE CASE PhD award NE/L002531/1 (Natural History Museum CASE Partner) to
- ADE, a Natural Environment Research Council-NIGFSC IP-1833-0618 award to ADE and
- DAHT, and a Royal Society University Research Fellowship (URF\R\231021) awarded to

- RMC. DAHT acknowledges a Royal Society Wolfson Research Merit Award (WM130051).
- Rachael H. James, Juerg M. Matter, M. Grace Andrews, Catriona D. Menzies, provided helpful
- 543 discussions on water sampling methods and analysis. For the purpose of open access, the author
- has applied a Creative Commons Attribution (CC BY) licence to any Author Accepted
- 545 Manuscript version arising
- 546
- 547 References
- Alt, J.C., Shanks III, W.C., Crispini, L., Gaggero, L., Schwarzenbach, E.M., Früh-Green, G.L.
- and Bernasconi, S.M., 2012. Uptake of carbon and sulfur during seafloor serpentinization
- and the effects of subduction metamorphism in Ligurian peridotites. Chemical Geology,
- 551 322, pp.268-277.
- Apollaro, C., Marini, L., Critelli, T., Barca, D., Bloise, A., DeRosa, R., Liberi, F., Miriello, D.
- 553 2011. Investigation of rock-to-water release and fate of major, minor, and trace elements
- in the metabasalt-serpentinite shallow aquifer of Mt. Reventino (CZ, Italy) by reaction
- path modelling. Appl. Geochem. 26: 1722-1740.
- Apollaro, C., Fuoco, I., Brozzo, G., Rosa, R.D., 2019. Release and fate of Cr(VI) in the
- ophiolitic aquifers of Italy: the role of Fe(III) as a potential oxidant of Cr(III) supported
- by reaction path modelling. Sci. Total Environ. 660, 1459–1471.
- Bloise, A., Fuocoa, I., Vespasianoa, G., Parisia, F., La Russaa, M.F., Piersantea, C., Perria, G.,
- Filicettia, S., Pacellad, A., De Rosaa, R., Apollaroa, C. 2024. Assessing potentially toxic
- elements (PTEs) content in asbestos and related groundwater: A review of the levels
- detected. Science of the Total Environment 955: 177116.
- Bullock, L.A., James, R.H., Matter, J., Renforth, P., Teagle, D.A.H., 2021. Global carbon
- dioxide removal potential of waste materials from metal and diamond mining. Frontiers
- in Climate 3.
- 566 Charalambides, A., Petrides, G., Pashalidis, I. 2003. Rainwater characteristics over an old
- sulphide mine refuse in Sha, Cyprus. Atmos. Environ. 37: 1921-1926.
- 568 Chavagnac, V., C. Monnin, G. Ceuleneer, C. Boulart, and G. Hoareau 2013. Characterization
- of hyperalkaline fluids produced by low-temperature serpentinization of mantle
- peridotites in the Oman and Ligurian ophiolites, Geochem. Geophys. Geosyst., 14, 2496–
- 571 2522, doi:10.1002/ggge.20147.
- 572 Christofi, C., Bruggeman, A., Kuells, C., Constantinou, C., 2020. Isotope hydrology and
- 573 hydrogeochemical modeling of Troodos Fractured Aquifer, Cyprus: the development of
- 574 hydrogeological descriptions of observed water types. Appl. Geochem. 123, 104780.

- 575 Craw, D., Landis, C.A., and Kelsey, P.I. 1987: Authigenic chrysotile formation in the matrix
- of Quaternary debris flows, northern Southland, New Zealand. Clays Clay Min. 35: 43-
- 577 52.
- Daghino, S., Turci, F., Tomatis, M., Girlanda, M., Fubini, B., Perotto, S. 2009. Weathering of
- 579 chrysotile asbestosby the serpentine rock inhabiting fungus Verticillium leptobactrum.
- 580 FEMS Microbiol. Ecol. 69: 132–141.
- Duivenvoorden, L.J., Roberts D,T., Tucker, G.M. 2017. Serpentine geology links to water
- quality and heavy metals in sediments of a stream system in central Queensland,
- Australia. Environ. Earth Sci. 76: 320.
- Ellison, E. T., Templeton, A. S., Zeigler, S. D., Mayhew, L. E., Kelemen, P. B., Matter, J. M.,
- & The Oman Drilling Project Science Party 2021. Low temperature hydrogen formation
- during aqueous alteration of serpentinized peridotite in the Samail ophiolite. Journal of
- Geophysical Research: Solid Earth, 126, e2021JB021981. https://doi.
- 588 org/10.1029/2021JB021981.
- 589 Emmanouil, K., Kalliopi, A., Dimitrios, K., Evangelos, G. 2009. Asbestos pollution in an
- inactive mine: Determination of asbestos fibers in the deposit tailings and water. Jour.
- 591 Hazard. Materials 167: 1080-1088.
- 592 Emmanuel, S. 2022. Modeling the effect of mineral armoring on the rates of coupled
- dissolution-precipitation reactions: Implications for chemical weathering. Chem. Geol.
- 594 601: 120868.
- Evans, A.D., Teagle, D.A.H., Craw, D., Henstock, T.J., Falcon-Suarez, I.H., 2021. Uplift and
- exposure of serpentinized massifs: Modeling differential serpentinite diapirism and
- exhumation of the troodos mantle sequence, Cyprus. J. Geophys. Res. Solid Earth 126.
- 598 https://doi.org/10.1029/2020jb021079.
- 599 Evans, A.D., Craw, D., Teagle, D.A.H. 2024a. Active near-surface mobilisation of slab-derived
- geochemical signatures by hyperalkaline waters in brecciated serpentinites. Chem. Geol.
- 601 643, 121822.
- 602 Evans, A.D., Standish, C.D., Milton, J.A., Robbins, A.G., Craw, D., Foster, G.L., Teagle,
- D.A.H. 2024b. Imaging of boron in altered mantle rocks illuminates progressive
- serpentinisation episodes. Geochem. Perspect. Letters 29: 20-25.
- 605 Evans, A.D., Cooper, M.J., Craw, D., Teagle, D.A.H., 2024c. Progressive leaching data of
- serpentinized mantle rocks from the Troodos Massif and Limassol Forest Complex,
- 607 Cyprus, Mendeley Data, V1, doi: 10.17632/x8chfn6nwt.1

- Evans, A.D., Cooper, M.J., Craw, D., Teagle, D.A.H., 2025. Multiple episodes of serpentinite
- alteration revealed by progressive leaching experiments. Geochim. Cosmochim. Acta (in
- 610 press).
- 611 Griggs, C., Pearson, C., Manning, S.W., Lorentzen, B. 2013. A 250-year annual precipitation
- reconstruction and drought assessment for Cyprus from Pinus brutia Ten. tree-rings. Int.
- 613 Jour. Climatology, DOI: 10.1002/joc.3869.
- 614 Gwenzi, W. 2020. Occurrence, behaviour, and human exposure pathways and health risks of
- toxic geogenic contaminants in serpentinitic ultramafic geological environments
- 616 (SUGEs): A medical geology perspective. Sci. Total Environ. 700: 134622.
- Jacques, O., Pienitz, R. 2022. Asbestos mining waste impacts on the sedimentological
- evolution of the Bécancour chain of lakes, southern Quebec (Canada). Sci. Total Environ.
- 619 807: 151079.
- Kelemen, P.B., Matter, J., 2008. In situ carbonation of peridotite for CO2 storage. Proc. Natl.
- 621 Acad. Sci. 105: 17295–17300.
- Kelemen, P.B., Matter, J., Streit, E.E., Rudge, J.F., Curry, W.B., Blusztajn, J., 2011. Rates and
- mechanisms of mineral carbonation in peridotite: Natural processes and recipes for
- enhanced in situ CO₂ capture and storage. Annu. Rev. Earth Planet. Sci. 39: 545–576.
- Kumar, A. Maiti, S.K. 2015. Assessment of potentially toxic heavy metal contamination in
- agricultural fields, sediment, and water from an abandoned chromite-asbestos mine waste
- of Roro hill, Chaibasa, India. Environ. Earth Sci. 74: 2617-2633.
- 628 Langmuir D. (1997) Aqueous Environmental Geochemistry. Prentice Hall, Upper Saddle River
- New Jersey, USA, 600 pp.
- 630 Lechat, K., Lemieux, J.-M., Molson, J., Beaudoin, G., H'ebert, R., 2016. Field evidence of
- 631 CO2 sequestration by mineral carbonation in ultramafic milling wastes, Thetford Mines,
- 632 Canada. Int. J. Greenh. Gas Control 47: 110–121.
- 633 Le Coz, M., Bruggeman, A., Camera, C., Lange, M.A. 2016. Impact of precipitation variability
- on the performance of a rainfall—runoff model in Mediterranean mountain catchments.
- 635 Hydrol. Sci. Jour. 61: 507-518.
- 636 Leong, J.A.M., Howells, A.E., Robinson, K.J., Cox, A., Debes II, R.V., Fecteau, K.,
- Prapaipong, P., Shock, E.L., 2021. Theoretical predictions versus environmental
- observations on serpentinization fluids: lessons from the Samail ophiolite in Oman. J.
- Geophys. Res. Solid Earth 126. https://doi.org/10.1029/2020jb020756.
- Lottermoser, B. 2010. Mine Wastes: Characterization, Treatment and Environmental Impacts.
- Springer, Berlin, 400 pp.

- Matthies, R., Aplin, A.C., Jarvis, A.P. 2010. Performance of a passive treatment system for
- net-acidic coal mine drainage over five years of operation. Sci. Total. Environ. 408:
- 644 4877-4885.
- Meck, M., Love, D., Mapani, B., 2006. Zimbabwean mine dumps and their impacts on river
- quality a reconnaissance study. Phys. Chem. Earth 31, 797–803.
- Moores, E.M., Vine, F.J., 1971. The Troodos Massif, Cyprus and other ophiolites as Oceanic
- crust: evaluation and implications. Philos. Trans. R. Soc. A Math. Phys. Eng. Sci. 268,
- 649 443–467.
- Morag, N., Haviv, I., Katzir, Y., 2016. From ocean depths to mountain tops: Uplift of the
- Troodos ophiolite (Cyprus) constrained by low-temperature thermochronology and
- geomorphic analysis. Tectonics 35: 622–637.
- Neal, C., Shand, P., 2002. Spring and surface water quality of the Cyprus ophiolites. Hydrol.
- Earth Syst. Sci. 6: 797–817.
- Oelkers, E.H., Declercq, J., Saldi, G.D., Gislason, S.R., Schott, J. 2018. Olivine dissolution
- rates: A critical review. Chem. Geol. 500: 1-19.
- Oskierski, H.C., Turvey, C.C., Wilson, S., Dlugogorski, B.Z., Altarawneh, M., Mavromatis,
- V., 2021. Mineralisation of atmospheric CO2 in hydromagnesite in ultramafic mine
- tailings insights from Mg isotopes. Geochem. Cosmochim. Acta 309: 191–208.
- Paulo C., Power, I.M., Zeyen, N., Wang, B., Wilson, S. 2023. Geochemical modeling of CO2
- sequestration in ultramafic mine wastes from Australia, Canada, and South Africa:
- Implications for carbon accounting and monitoring. Appl. Geochem. 105630.
- Plumper, O., Beinlich, A., Bach, W., Janots, E., Austrheim, H. 2014. Garnets within geode-
- like serpentinite veins: Implications for element transport, hydrogen production and life-
- supporting environment formation. Geochim. Cosmochim. Acta 141: 454-471.
- Ross, M., Nolan, R.P. 2003. History of asbestos discovery and use and asbestos-related disease
- in context with the occurrence of asbestos within ophiolite complexes. Geol. Soc.
- 668 America Spec. Paper 373: 447-470.
- 669 Scambelluri, M., Piccardo, G.B., Phillipot, P., Robbiano, A., Negretti, L. 1997. High salinity
- fluid inclusions formed from recycled seawater in deeply subducted alpine serpentinite.
- Earth. Planet. Sci. Letters 148: 485-499.
- Thom, J.G.M., Dipple G.M., Power, I.M., Harrison, A.L. 2013. Chrysotile dissolution rates:
- 673 Implications for carbon sequestration. Appl. Geochem. 35: 244-254.
- Wilson, R.A.M., 1959. The Geology of the Xeros-Troodos Area (No. 1). Authority of the
- Government of Cyprus.

Wilson, S.A., Dipple, G.M., Power, I.M., Thom, J.M., Anderson, R.G., Raudsepp, M., Gabites, J.E., Southam, G., 2009. Carbon dioxide fixation within mine wastes of ultramafic hosted ore deposits: examples from the Clinton Creek and Cassiar chrysotile deposits, Canada. Econ. Geol. 104: 95–112.

Tables

Table 1. Analysis of evolved surface water sample BU1 from the Amiantos asbestos mine, Troodos ophiolite, Cyprus (Fig. 1a,b), showing the range of light elements that is the focus of this study. EC = electrical conductivity. DIC = dissolved inorganic carbon; *recalculated as HCO_3^- . A full set of analyses is provided in Supp. Table S1.

SAMPLE BU1 MINE WATER

	Tailings seepag	ge					
pН	8.7						
EC	1682	μS/cm					
8 180	-7.0	per mil					
δ D	-36.6	per mil					
Major comp	Major components						
	µmol/kg	mg/L					
Na^+	5799.7	133.3					
K ⁺	252.5	9.9					
Ca^{2+}	117.7	4.7					
Mg^{2+}	6577.1	159.9					
Cŀ	6370.5	225.9					
SO ₄ ²⁻	151.1	14.5					
DIC	10080.1	615*					
Si	168.5	4.7					

Minor and	trace	components
-----------	-------	------------

	µmol/kg	$\mu g/L$
Al	0.83	22.4
В	99.81	1079.0
Ba	0.37	50.6
Br	97.50	7.8
Cs	0.68	89.7
Cr	0.83	43.4
Fe	4.50	251.3
Li	16.96	117.7
Mn	0.13	7.1
Pb	0.00005	0.011
Rb	0.42	35.8
Sr	0.16	13.8

Minerals in rocks & tailings	Amount
Serpentine (Mg±Fe ²⁺), incl. chrysotile	>95%
Ca-Mg carbonates ($\pm Fe^{2+}$)	Common
Magnetite (Fe ²⁺ & Fe ³⁺)	Minor
Pyrrhotite (Fe ²⁺)	Rare
Andradite (Ca, Fe ³⁺)	Minor
Ferric oxyhydroxide (Fe ³⁺)	Trace
Tailings water BU1 potential minerals	Log Q/K
Sepiolite (Mg)	+5.83
Chrysotile (Mg)	+5.62
Dolomite (CaMg)	+3.91
Huntite (MgCa)	+3.91
Magnesite (Mg)	+1.68
Calcite (Ca)	+0.68
Aragonite (Ca)	+0.44
Hydromagnesite (Mg)	-0.15
Monohydrocalcite (Ca)	-0.39
Nesquehonite (Mg)	-1.01
Amorphous silica (Si)	-1.10
Brucite, Mg(OH) ₂	-1.50
Gypsum (Ca)	-4.03
Epsomite (Mg)	-4.86
Halite (Na)	-6.16
Sylvite(K)	-6.89

Figures

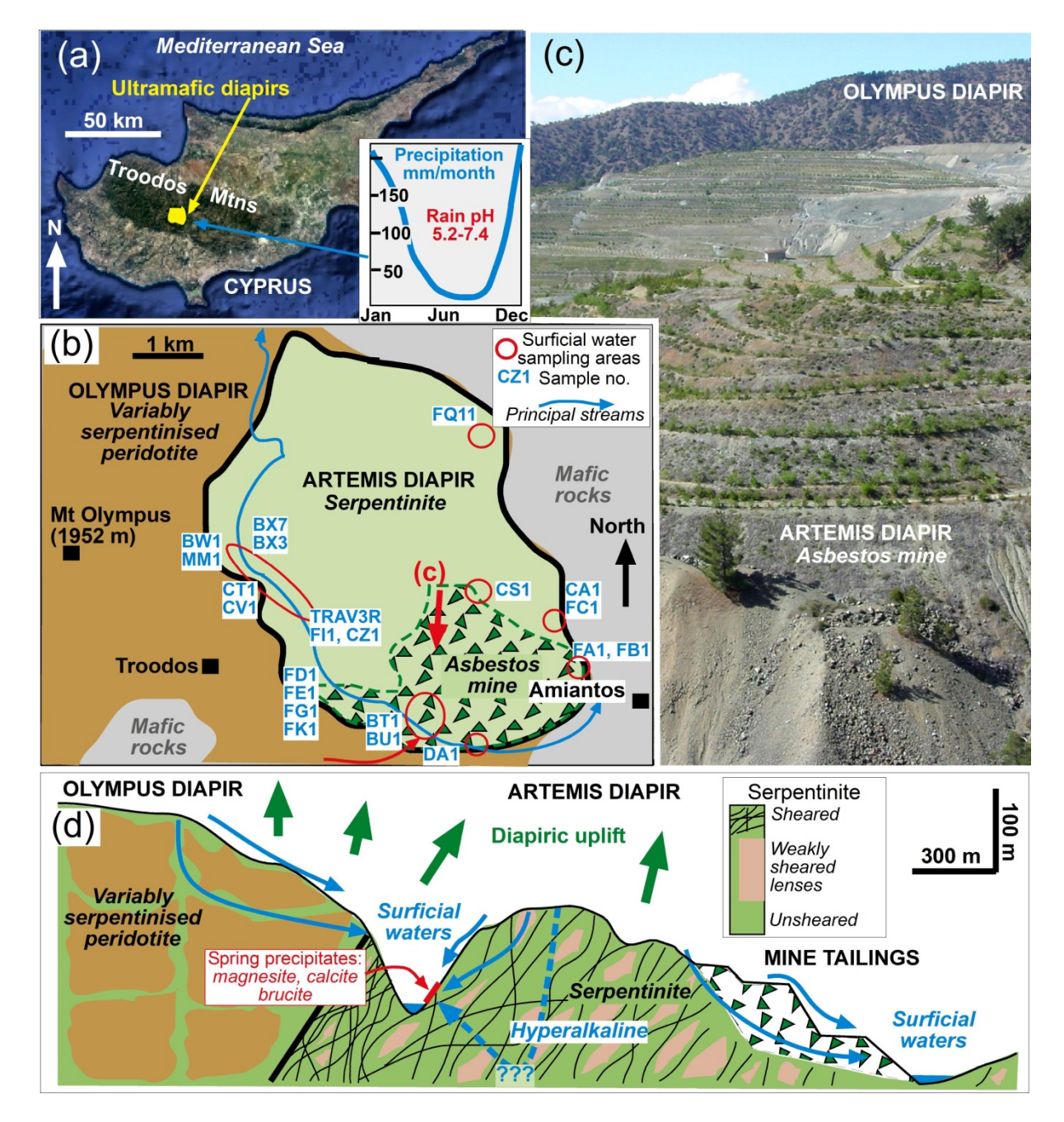


Fig. 1. Location and hydrogeological context for the Amiantos asbestos mine. (a) Map of Cyprus (from GoogleEarth) showing the forested Troodos Mountains and the location of the ultramafic diapirs in this study. Inset shows rainfall data for mountain crest (Charalambides et al. 2003; Griggs et al. 2013). (b) Sketch geological map of the Artemis Diapir (simplified from Evans et al. 2021) with the asbestos mine footprint and associated water sampling areas. (c) General view across the asbestos mine (as indicated in b) in 2010, with early stages of site revegetation. (d) Cartoon composite cross section showing structural and lithologic relationships of the two ultramafic diapirs, with depictions of surficial water flow relevant to this study.

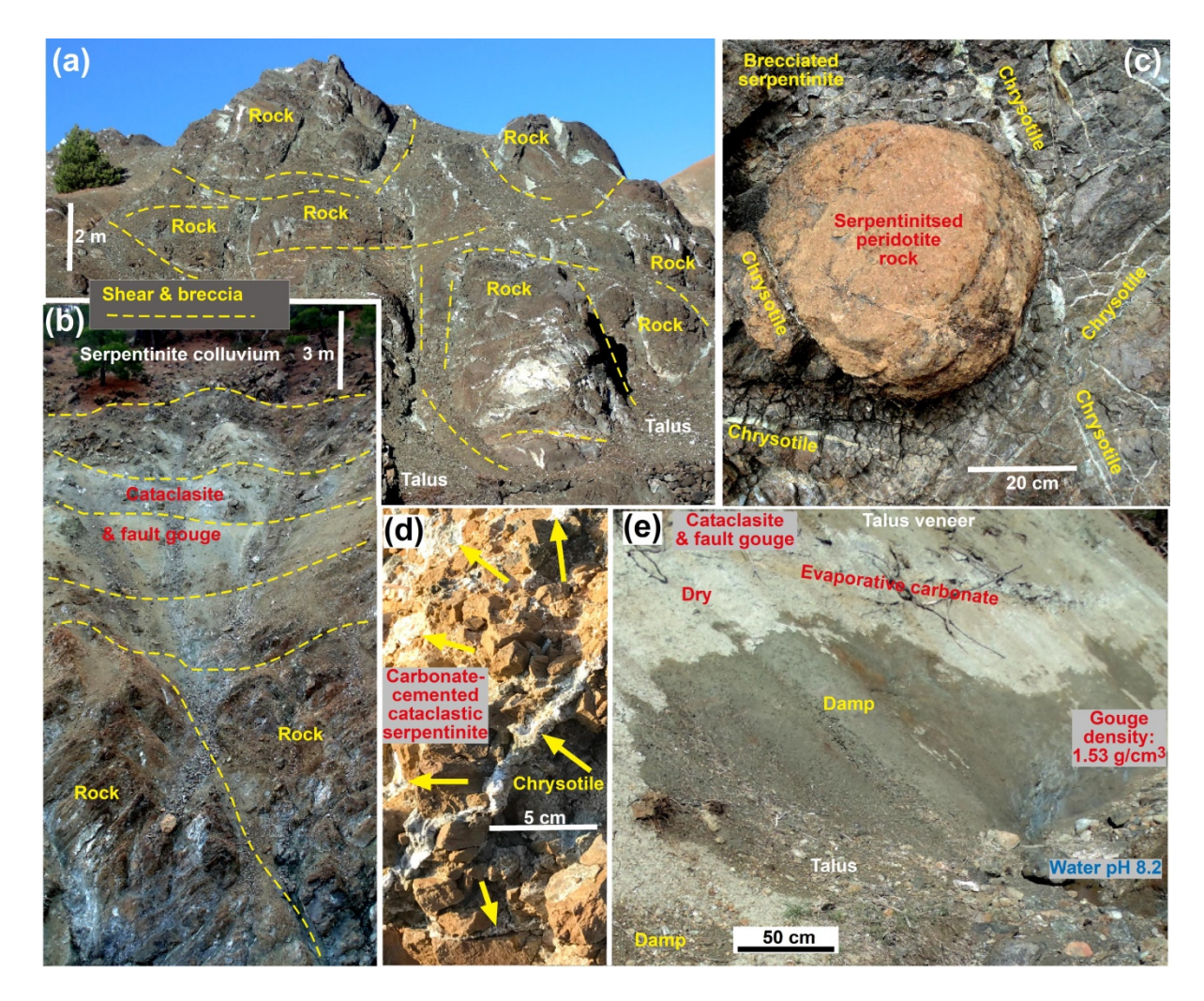


Fig. 2. Structure and lithology in Artemis Diapir host rocks for the asbestos mine. (a) Typical view of unmined serpentinite landscape, with blocks of relatively competent rock surrounded by variably sheared, brecciated and veined rock. White veins are all serpentine minerals with minor carbonate. (b) Steep active erosional scar in an unmined valley wall, showing contrasts between relatively competent rock blocks and fine grained sheared cataclasite and fault gouge. (c) Natural outcrop view of competent serpentinite core surrounded by variably veined brecciated serpentinite. (d) Outcrop near mine of carbonate-cemented and carbonate-veined serpentinite cataclasite and breccia, cut by late-stage chrysotile veins (yellow arrows; context in Supp. Fig. S2). (e) Road cut outside mine through serpentinite cataclasite and gouge in major shear zone at western diapir margin (Fig. 1b.d). Slow water seepage causes partial dampness. Density from Evans et al. (2021).

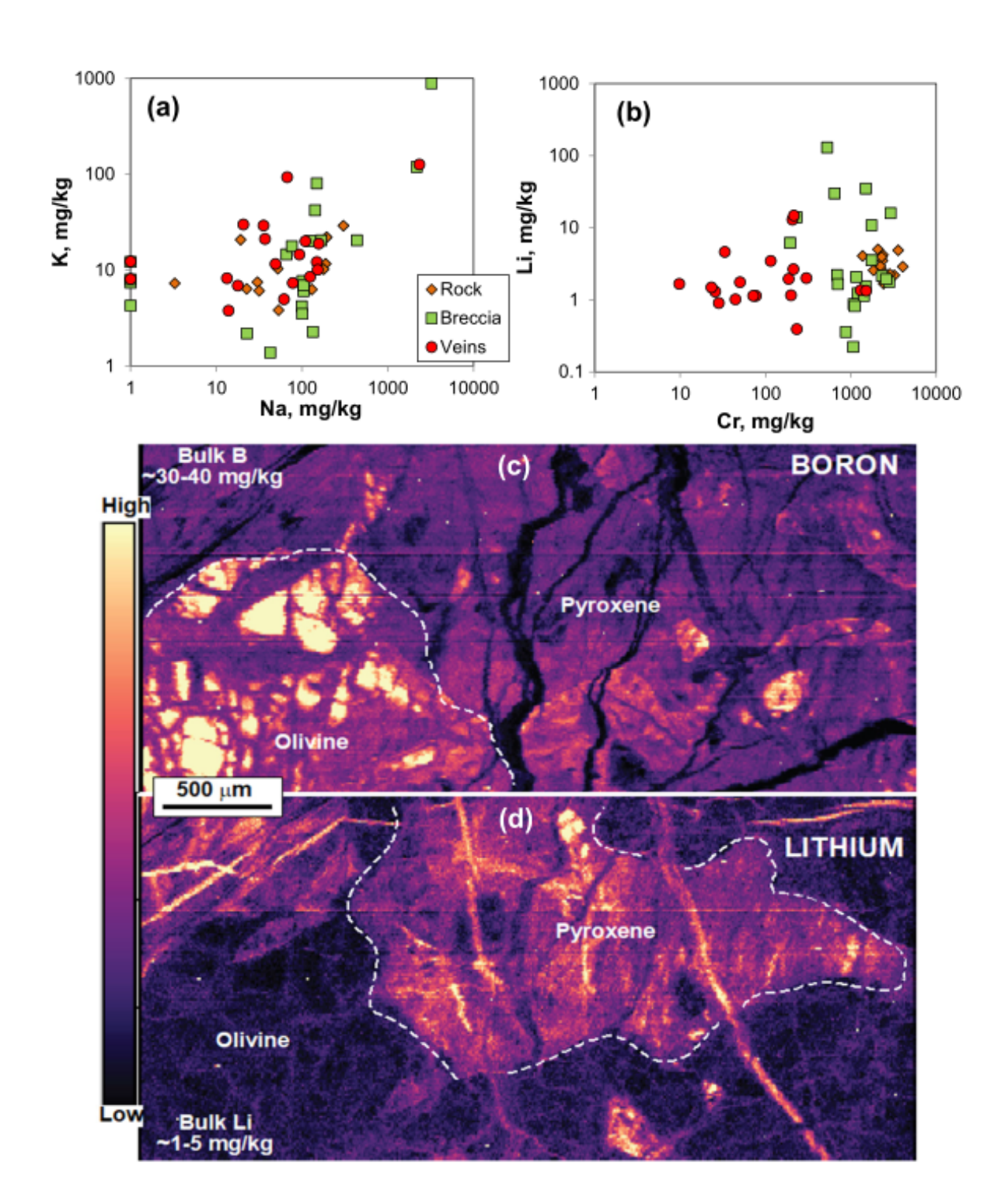


Fig. 3. Examples of rock trace element variations in Artemis Diapir (data from Evans et al. 2024b; 2025). (a) Na and K contents in rocks (serpentinised peridotite), serpentinite breccias, and serpentine veins including chrysotile veins. (b) Cr and Li variations in same materials as in a. (c) Laser ablation ICP-MS map of B distribution in a serpentinised peridotite sample (modified after Evans et al. 2024b). (d) Li distribution map in same rock as in c. Black seams in c are serpentine veins that have low B but detectable Li.

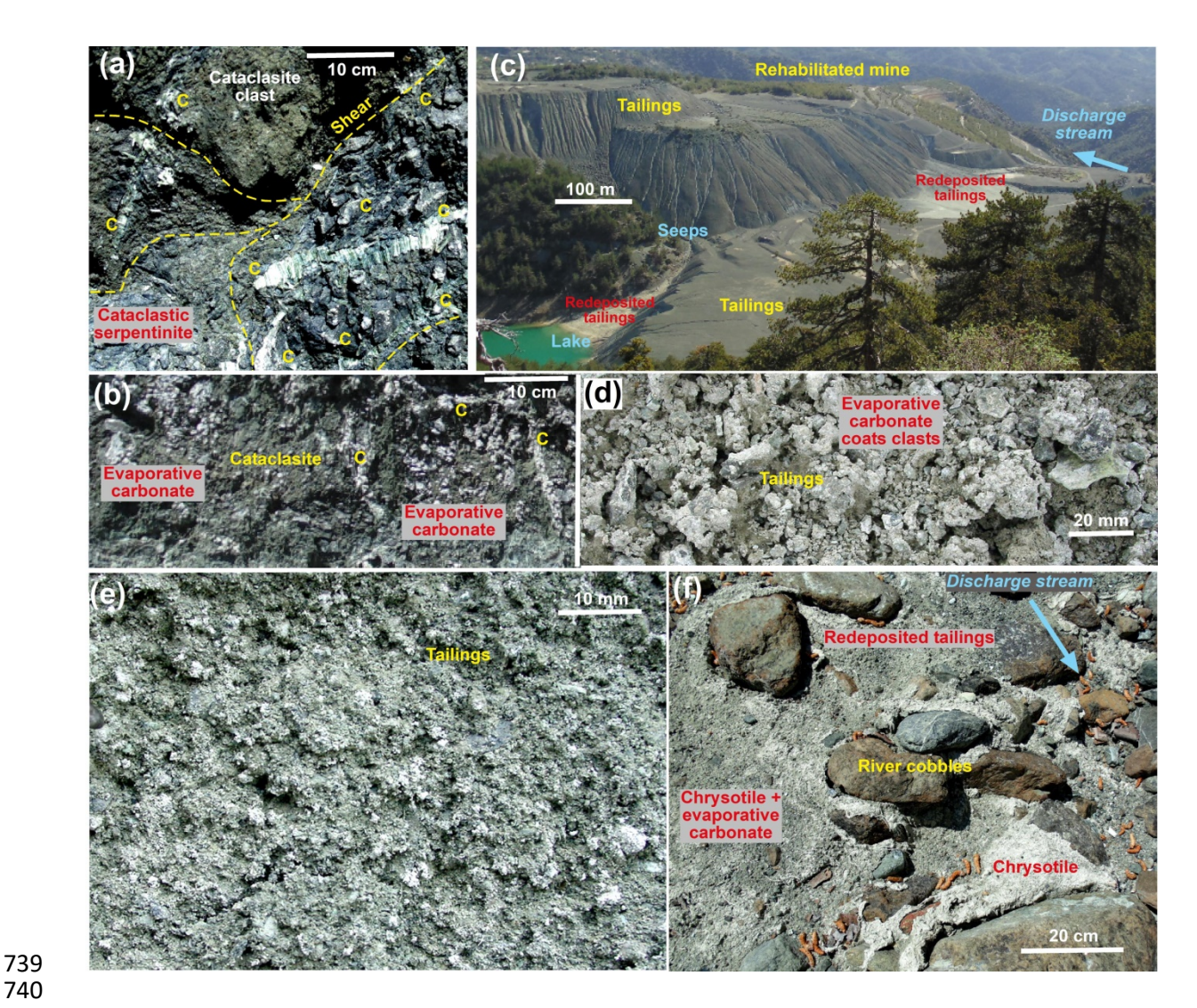


Fig. 4. Asbestos mine and tailings. (a,b) Mine outcrops of sheared and cataclastic serpentinite with abundant chrysotile veins (C) that have been disrupted by on-going deformation. White surface coatings in b are evaporative carbonate. (c) General view of a large tailings pile that has not undergone rehabilitation. Water samples were collected from lake, a seep, and discharge stream, as well as the natural stream feeding the lake. (d) Tailings with abundant evaporative carbonate (white) coating angular fragments of serpentinite. (e) Close view of a fresh outcrop of tailings. White material is chrysotile, other serpentine vein fragments, and some carbonate. (f) Stream bed down-valley from tailings, with redeposited tailings, white mats of accumulated chrysotile, and white surficial evaporative carbonate coatings.

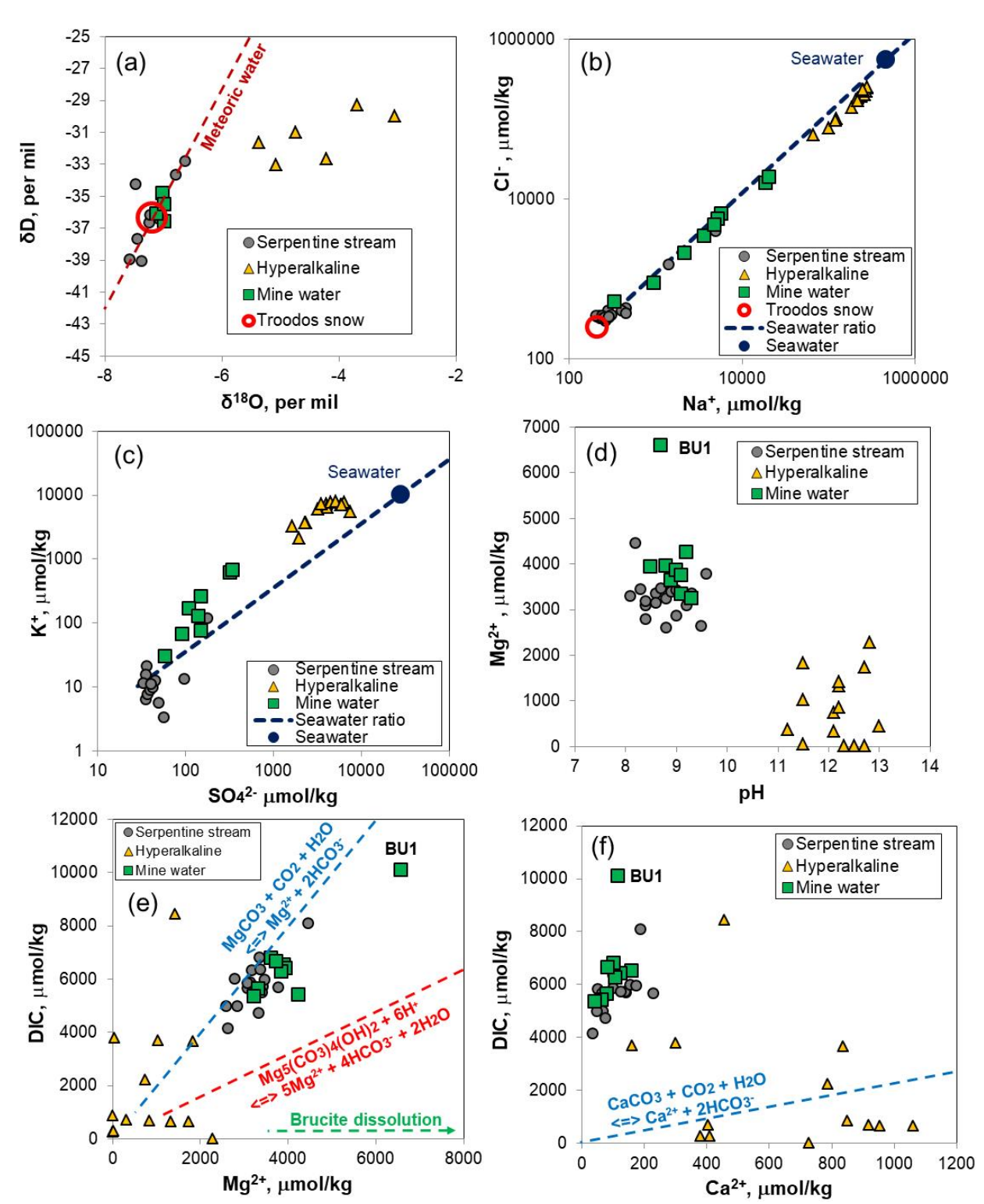


Fig. 5. Principal components of water compositions in Artemis Diapir and Amiantos asbestos mine. (a) Oxygen and hydrogen stable isotopes. Local Cyprus meteoric water line is from Christofi et al. (2020). (b) Na⁺ and Cl⁻ in relation to seawater and the seawater Na/Cl molar ratio. (c) K⁺ and sulfate in relation to seawater and the seawater K/sulfate molar ratio. (d) Water pH and Mg²⁺ concentrations. (e) Mg²⁺ versus dissolved inorganic carbon (DIC), in relation to the stoichiometric equations for dissolution of magnesite and hydromagnesite. (f) Ca²⁺ versus DIC in relation to stoichiometric equation for dissolution of calcite.

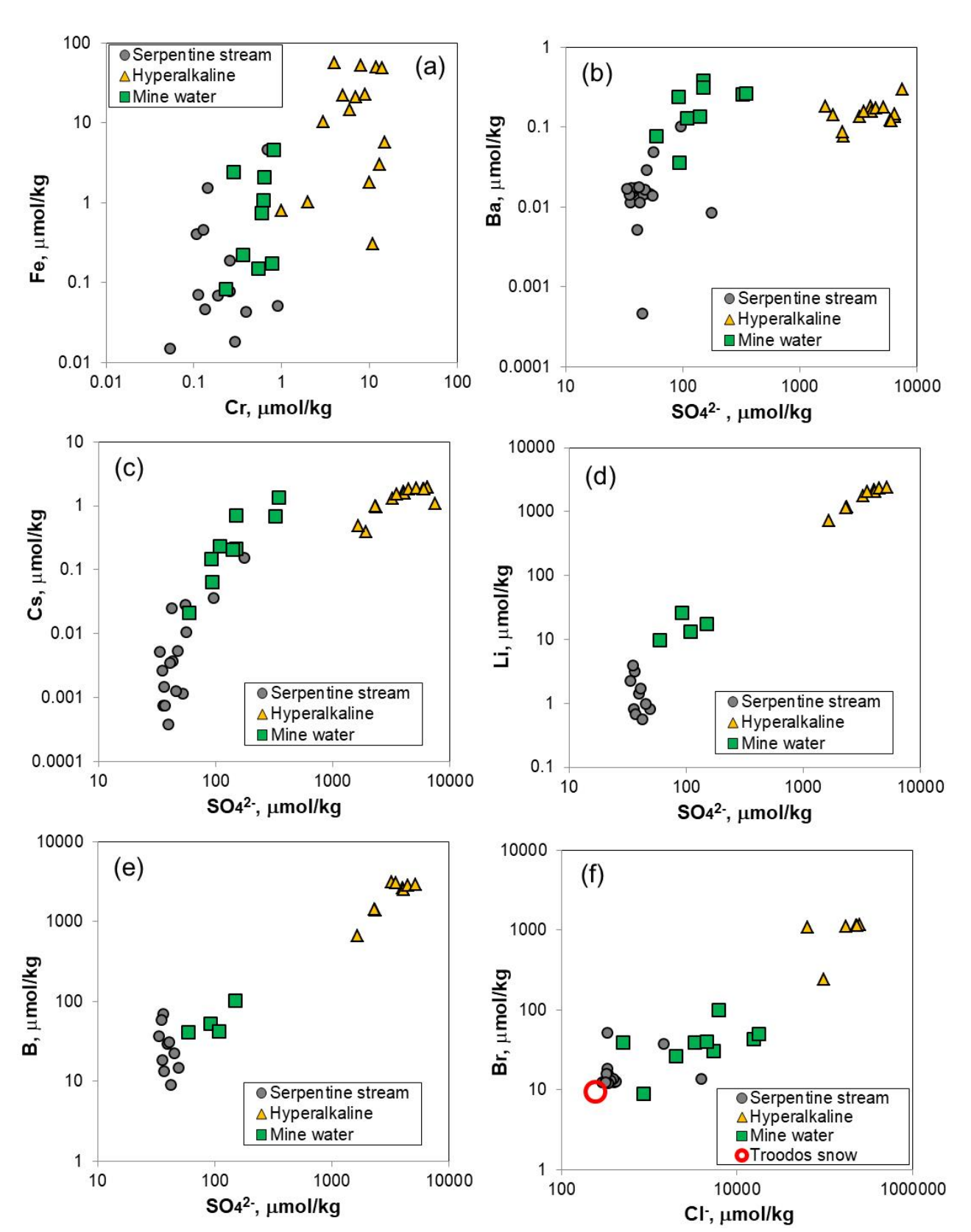


Fig. 6. Minor and trace elements in waters of Artemis Diapir and Amiantos mine. (a) Fe versus Cr. (b) Sulfate versus Ba. (c) Sulfate versus Cs. (d) Sulfate versus Li. (e) Sulfate versus B. Cl versus Br.

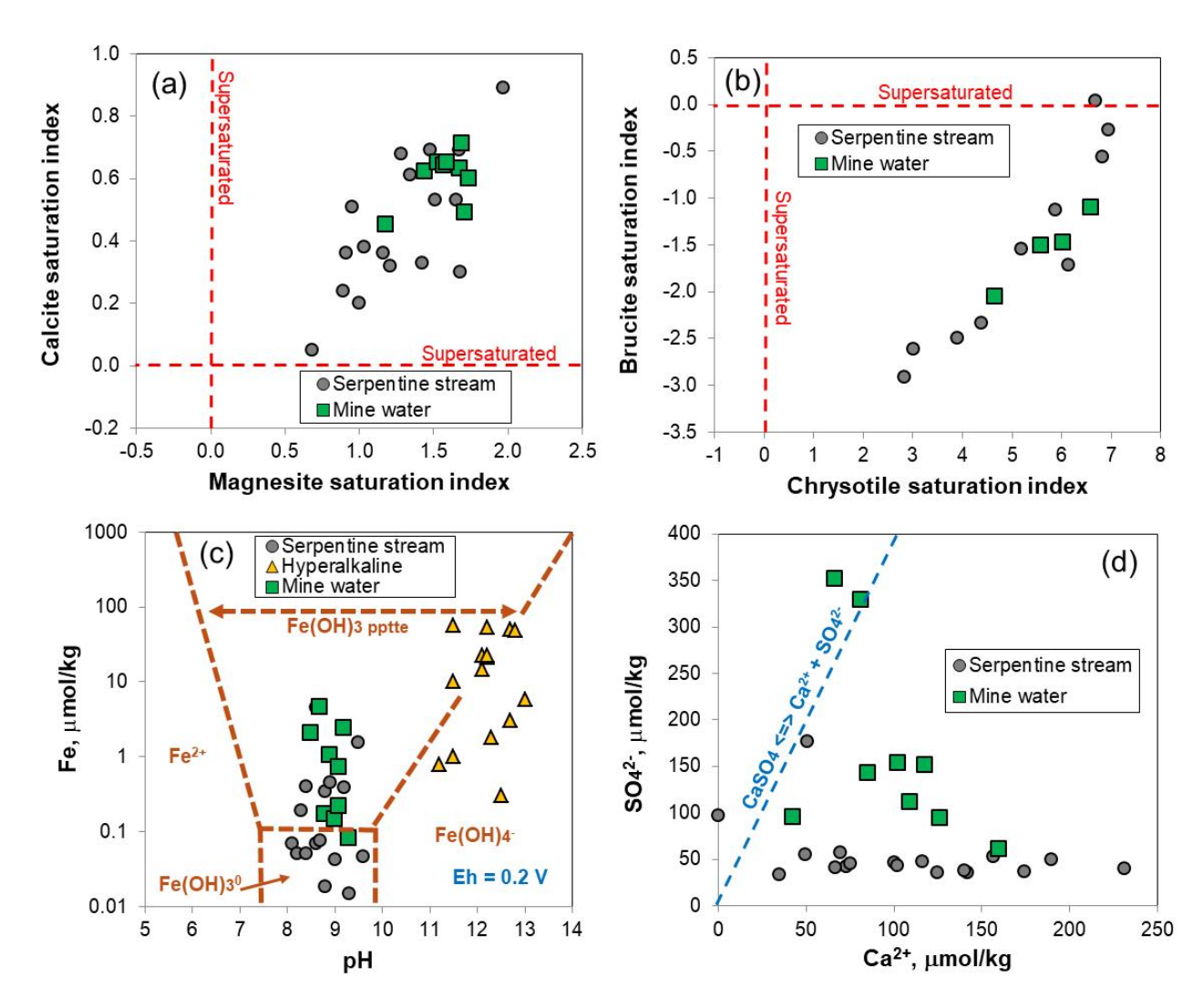


Fig. 7. Mineral dissolution in Artemis Diapir waters. Saturation indexes, calculated by Geochemists Workbench at 25°C using SpecE8 for magnesite and calcite (a) and chrysotile and brucite (b). (c) Fe speciation in relation to pH at Eh of 0.2 V, calculated using ACT2. (d) Ca²⁺ versus sulfate in relation to stoichiometric gypsum dissolution or precipitation.

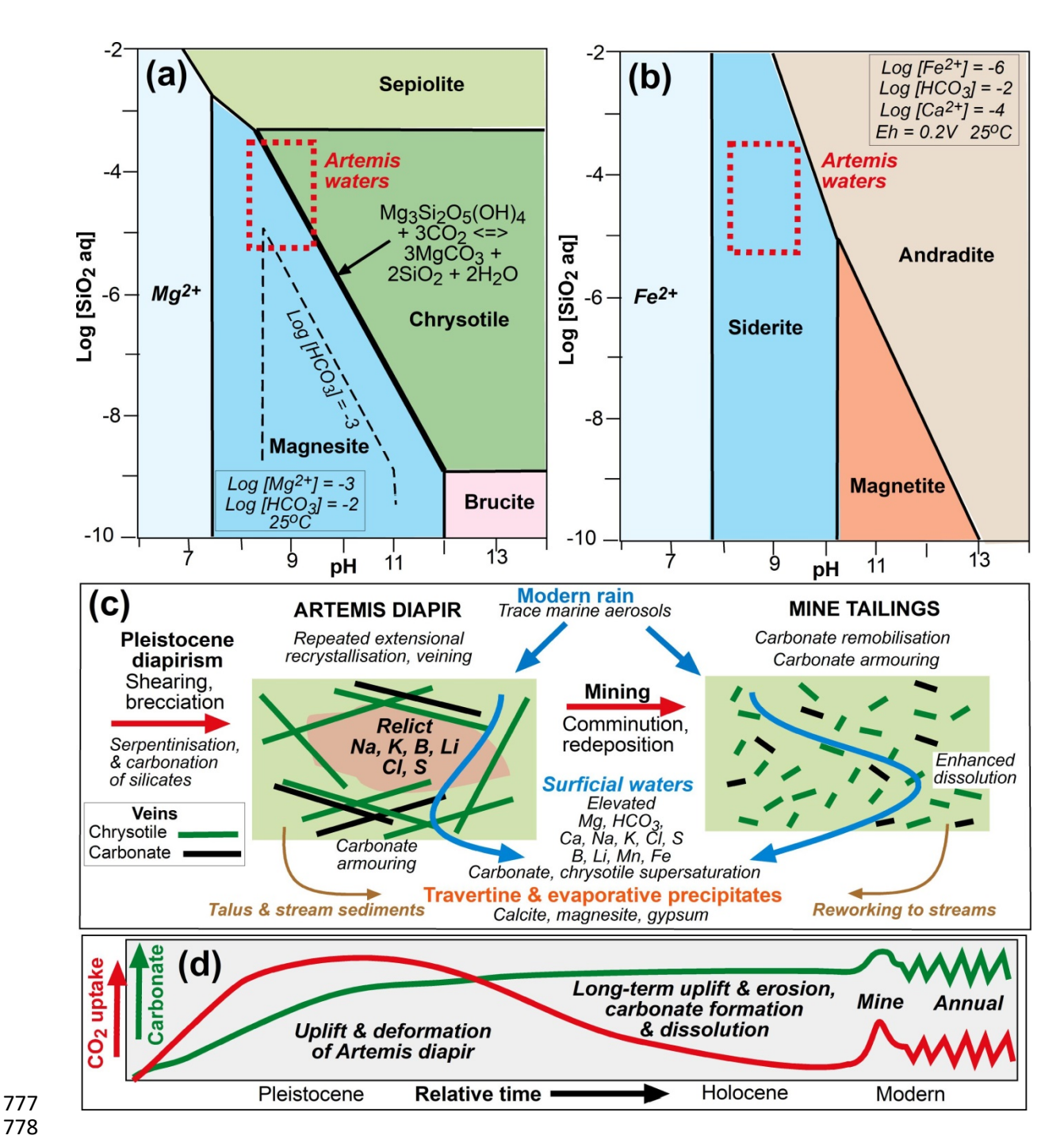


Fig. 8. Geochemical models and summary sketches. (a) Phase diagram (from Geochemists Workbench, ACT2) depicting equilibrium relationships among principal Mg minerals for water compositions around the Amiantos asbestos mine. A simplified reaction for CO₂ sequestration via carbonation of chrysotile is indicated. (b) Phase diagram (as for a) for iron minerals. (c) Sketch showing the principal processes and products in the Artemis Diapir during uplift and deformation followed by mine tailings production. (d) Schematic depiction of CO₂ uptake into carbonates and subsequent amounts of carbonates in Artemis Diapir over relative time. Annual changes since mining are exaggerated for illustrative purposes, and were also a long-term feature of the system.